

Synthesis and Characterization of Hybrid Films from Hyperbranched Polyester Using a Sol-Gel Process

Amélie Houel, Jocelyne Galy, Aurélie Charlot, Jean-François Gérard

Université de Lyon, CNRS, UMR 5223, INSA-Lyon, Ingénierie des Matériaux Polymères, F-69621 Villeurbanne, France

Correspondence to: J. Galy (E-mail: jocelyne.galy@insa-lyon.fr)

ABSTRACT: Hybrid organic/inorganic materials were prepared by an *in situ* sol-gel process using tetraethoxysilane (TEOS) in the presence of hyperbranched polyester. The influences of hyperbranched polyester molar mass as well as the amount of TEOS were examined. The condensation degree was characterized by solid state ^{29}Si NMR. The combination of solubility tests, calcination tests, SAXS and dynamic mechanical analysis allowed us to investigate the hybrid material nanostructure. The results show high compatibility between the inorganic silica phase and the organic polymer phase, due to the spherical shape of the hyperbranched polymer and its numerous hydroxyl groups. As a consequence, a continuous inorganic phase was formed even with a low silica precursor content without any macroscopic phase separation. These hybrid materials have a high T_g and high storage modulus even at an elevated temperature combined with improved thermal stability. © 2013 Wiley Periodicals, Inc. *J. Appl. Polym. Sci.* **2014**, *131*, 39830.

KEYWORDS: coatings; dendrimers; hyperbranched polymers and macrocycles; morphology; nanostructured polymers; properties and characterization

Received 6 June 2013; accepted 8 August 2013

DOI: 10.1002/app.39830

INTRODUCTION

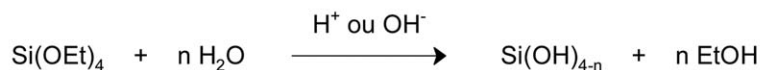
In coating applications, advanced properties and multifunctionality are essential to match increased market demand. These functionalities can be abrasion and scratch resistance, gloss, toughness, mechanical properties, barrier properties, self-healing and self-cleaning, corrosion resistance, etc. In this context, polymer-based organic-inorganic (O/I) nanomaterials have attracted a great deal of attention in recent decades because a synergistic combination of the properties of each phase is expected from the nanolevel.¹

These materials can be obtained *via* different routes: (i) by the addition of preformed nanoparticles or nanoclusters, the most significant examples being layered silicates, silicas, nanotube-like or needle-like metal oxides, or polyhedral oligomeric silsesquioxane (POSS),²⁻⁷ (ii) by *in situ* generation of an inorganic-rich phase through a conventional sol-gel process involving hydrolysis and condensation reactions under mild conditions, starting from hydrolysable metal alkoxides, generally alkoxy silanes.⁸⁻¹² These reactions are illustrated in Scheme 1 for tetraethoxysilane (TEOS), often used for the formation of hybrid materials. Using the sol-gel process makes it possible to grow an inorganic phase into an organic polymeric matrix from a reaction-induced phase separation mechanism, allowing a very fine dispersion of the inorganic phase even at the molecular level. The nanostructure obtained depends on many parameters,

such as the chemical nature of each phase and the conditions of synthesis. Hybrid materials are generally divided into two categories according to the nature of the O/I interface: the noncovalent O/I composites and the covalent composites corresponding to “class I” and “class II” hybrids,¹³ respectively, in the categories defined by Sanchez and Ribot.¹⁴ Non-covalent composites refer to materials in which interactions between the two phases consist of noncovalent interactions due to van der Waals, electrostatic and hydrogen bonding forces. Covalent hybrids are usually obtained *via* two routes: in the first, a polymer bearing $-\text{Si}(\text{OR})_3$ group is subjected to hydrolysis and condensation in the presence of an alkoxy silane such as $\text{Si}(\text{OR})_4$ in a homogeneous solution, whereas in the second route, an organofunctional alkoxy silane, denoted as a coupling agent, is used to provide covalent bonds at the interface between inorganic and organic-rich phases.

Numerous organic-inorganic hybrids based on linear polymers and thermosetting polymers have been examined in literature. However, only a few studies have been reported on hybrids based on polyesters, either linear, unsaturated or hyperbranched polyesters.^{13,15-27} Ester groups in polyester chains are not strong enough to form hydrogen bonds with silanols,¹⁷ so the use of a type of polyester which contains hydroxyl groups is of a great interest to increase the interfacial forces between the polymer and the silica network. Frings et al.¹⁵ studied a linear hydroxy

Hydrolysis:



Condensation :

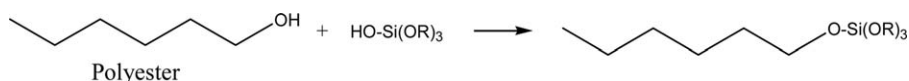


Scheme 1. Sol-gel reactions of tetraethoxysilane.

terminated polyester—TEOS system, catalyzed by *p*-toluenesulfonic acid monohydrate. A transparent material was obtained with increased hardness. The authors concluded that the interactions between the polyester and hydrolyzed TEOS probably take place via condensation of the hydroxyl groups as shown in Scheme 2. In another study,¹⁶ the authors used a trifunctional hydroxy-terminated polyester, hexakis(methoxymethyl)melamine as the crosslinking agent and prehydrolyzed TEOS (under acidic conditions). Above 11 wt % silica, the coatings appeared hazy. Round silica particles were observed by electron microscopy, with increasing size from 100 to 500 nm upon rising the amount of silica. This unexpected result was explained by the poor compatibility and lack of interactions between the O and I phases, causing phase separation. Hsu synthesized hybrid materials from a hydroxy-containing linear polyester and prehydrolyzed TEOS (under acidic conditions) mixed in THF.¹⁷ Transparent and flexible hybrids were obtained even at a high silica content (>40 wt %). The interfacial force, i.e., hydrogen bonding between the polyester and residual silanol of silica, was investigated by infrared spectroscopy. After heat treatment, this interfacial force changed into covalent bonds through dehydration of hydroxyl groups in polyester with residual silanols. The existence of covalent Si—O—C bonds was demonstrated by ²⁹Si NMR; *T_g* and thermal stability of the resulting materials were increased while the solubility was decreased.

To have more hydroxyl groups available, hyperbranched polyesters have also been used to prepare hybrid materials. Hyperbranched polymers (HBPs) possess special and unique properties, such as greater solubility in organic solvents and lower melting viscosity than their linear homologues; their highly branched structure gives access to a large number of reactive end groups. Moreover, their synthesis is relatively easy. This is why HBPs have been used in various coating and thermoset applications in order to improve properties such as processability or toughness. However, little work has been performed to prepare hybrids. Zou et al. used a modified hyperbranched polyester and a coupling agent, condensed with prehydrolyzed TEOS (under acidic conditions) to prepare hybrids.¹⁹ Transparent and hard materials were obtained.

FTIR evidenced the formation of chemical bonds between HBP and silica. SEM images showed well-dispersed particles of colloidal silica with a size of 6–9 nm. In another paper,²⁰ the same authors compared a linear acrylated polyester to a hyperbranched polyester. In both cases, a coupling agent and prehydrolyzed TEOS were used as the inorganic component. Hybrid materials were obtained via a sol-gel process and photopolymerization. In the films based on the HBP, the particle size was about 1–5 μm, while for linear polyester-based hybrids, agglomeration of silica particles was observed with particle sizes of 40–100 μm. These results were related to the good or poor miscibility of the organic phase with the inorganic one, respectively. Amerio et al. used an epoxy-functionalized HBP, modified or not by a coupling agent, and TEOS to prepare hybrid coatings.²⁴ The organic network was obtained by photopolymerization, initiated by a Brønsted acid. Then subsequent hydrolysis and condensation reactions were performed in an oven at 75°C for 4 h with constant humidity. No macroscopic phase separation was observed, and the materials were optically transparent. Silica domains were embedded in the polymeric matrix on the nanometer scale of 2–3 nm. In the absence of a coupling agent, the silica particles tended to agglomerate. Di Gianni et al. used either a phenol-terminated or an alkoxysilane-terminated HB polyester and Ti(iOPr)₄ as the inorganic precursor to prepare nanocomposites based on TiO₂ nanoparticles.²⁵ The polymer was cured by a diisocyanate. Hard and individual particles were observed by TEM, which were much smaller when the alkoxy-modified polymer was used as the matrix. SAXS measurements indicated that the interface was sharp in the case of the modified polymer and smooth in the case of the OH-terminated HB polyester. When TiO₂ was present, an increase in *T_g* was observed in the case of the unmodified OH-terminated polymer, while no *T_g* was detectable when the alkoxy silane-terminated polyester was used as the matrix. The authors explained this result by the formation of strong interactions between the modified polymer and the inorganic particles which strongly limited the mobility of the chains and shifted *T_g* near the decomposition temperature. The presence of TiO₂ enhanced the thermal stability as well as the hardness of the hybrid material.



Scheme 2. Reactions of hydroxyl-terminated polyester and hydrolyzed TEOS.

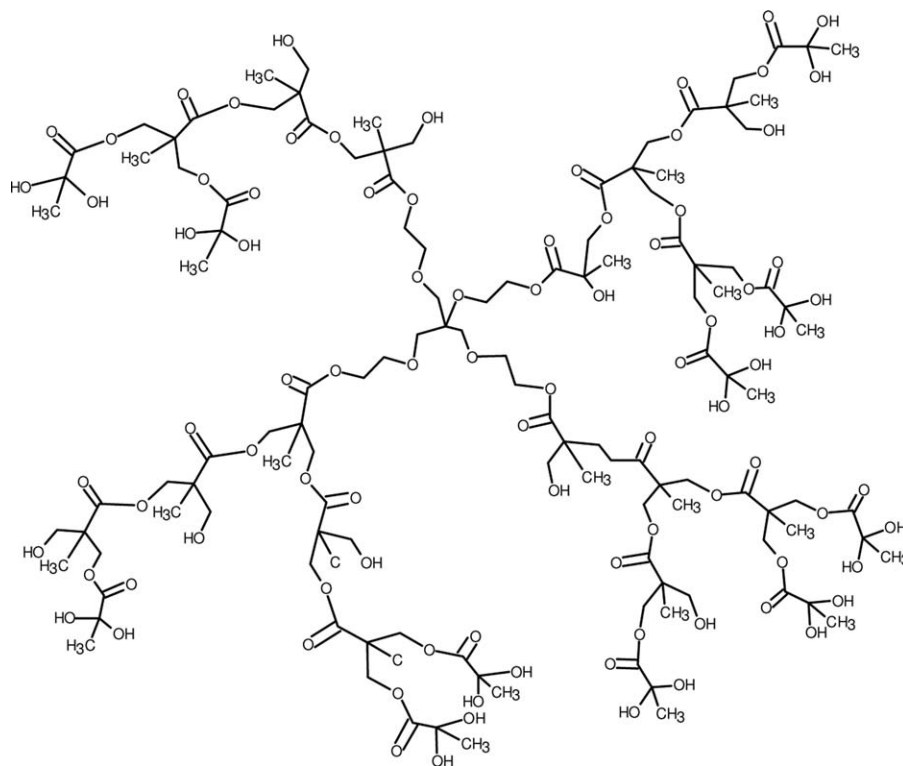


Figure 1. Schematic structure of H40.

In this study, the peculiar shape of HBPs was exploited for the synthesis of hybrid organic–inorganic materials, because of the numerous interactions allowed between the organic and inorganic phases. In particular, hydroxyl functionalized hyperbranched polyesters were used as the organic phase for film preparation. The inorganic phase was generated *in situ* from hydrolysis and condensation reactions of tetraethoxysilane, without addition of any coupling agent. Two series of hybrid materials were synthesized with different silica contents and a different polymer molar mass; they were characterized according to morphology, thermal and mechanical properties.

EXPERIMENTAL

Materials

Tetraethoxysilane (TEOS) was purchased from Sigma–Aldrich; dioxane and hydrochloric acid were purchased from Carlo-Erba SDS. The hyperbranched polyester Boltorn® H20 was obtained from Perstorp; it has theoretically 16 hydroxyl groups and a molecular weight, M_w , close to 1700 g mol^{-1} . The hyperbranched polyester PHF-64-OH® was purchased from Polymer Factory; it has theoretically 64 hydroxyl groups and a molecular weight, M_w , close to 7300 g mol^{-1} . A schematic structure of the H40 hyperbranched polyester is represented in Figure 1.

Synthesis of the Hybrid Materials

The hybrid materials were prepared using a protocol inspired by the work of Zou et al.¹⁹ A typical experiment procedure was the following: a glass reactor was charged with dioxane and polyester, with a concentration of 20 wt %, and heated to 90°C until a homogeneous mixture was obtained. The polyester was previously dried at 70°C for 24 h. Then, TEOS was progressively

added. Hydrolysis and condensation reactions were performed by adding an acidic water solution, at pH 2, using one equivalent of water per hydrolysable group, i.e., four in the case of TEOS. The mixture was kept under stirring at 90°C for 4 h. After a concentration step by evaporation at 50°C , the resulting solutions were applied on anti-adhesive coated glass plates. The materials were subsequently heated in an oven to 180°C at $4.3^\circ\text{C min}^{-1}$ followed by 4 h at 180°C . Free standing films of about $100 \mu\text{m}$ in thickness were thus obtained.

Different compositions were prepared to evaluate the impact of inorganic phase content and of the polyester molecular weight. The different compositions studied are named as follows: first the name of the polymer, H40 or H20, then the theoretical amount of equivalent SiO_2 in wt % calculated from the initial content of TEOS introduced in the reaction medium (Table I).

Characterization

Solid state CP-MAS ^{29}Si NMR spectra were recorded on a Bruker DSX 300 solid-state spectrometer. To determine the content of hyperbranched polyester incorporated into the silica network, hybrids were subjected to extraction with tetrahydrofuran (THF) for 72 h at room temperature. The organic phase was

Table I. Composition of the Different Hybrid Formulations

Wt % SiO_2	20	10	5
H20/H40 (g)	48	67.4	81
TEOS (g)	38.5	24.4	14
H_2O (g)	13.5	8.2	5

also removed from the hybrid sample by calcination under air at 300°C for 52 h to identify the nature of the continuous phase, organic vs. inorganic. The weight percentage of inorganic phase in hybrid materials was determined by thermogravimetric analysis (TGA) using Q500 form TA instruments. Samples were heated under air over the range 30–700°C at a heating rate of 10°C min⁻¹. Transmission electron microscopy (TEM) was performed on a Philips CM120 microscope. Thin sections, nominally 70 nm, were cut by a diamond knife using an ultramicrotome.

Small angle X-ray scattering (SAXS) experiments were performed using a pinhole camera (Molecular Metrology SAXS system) attached to a microfocussed X-ray beam generator (Osmic MicrMax 002) operating at 45 kV and 0.66 mA (30 W). The scattering intensities were considered on absolute scale using a glassy carbon standard.

A dynamic mechanical analysis (DMA) was carried out using a Rheometrics RSAII, at a frequency of 1 Hz in the tensile configuration, with strain amplitude of 0.03%. The storage modulus, E' , and the loss factor, $\tan \delta$, were measured from -50 to 300°C at a heating rate of 3°C min⁻¹ with a sample dimension of 30 × 11 × 0.1 mm³.

RESULTS AND DISCUSSION

Characterization and Structure of the H40-20 Film

First of all, we investigated the structure of the H40-20 hybrid film; it was synthesized from polyester H40 and an amount of TEOS leading to a theoretical content of 20 wt % of equivalent SiO₂.

The TEOS condensation state was quantified by solid-state ²⁹Si NMR, using a film sample after the final thermal treatment at 180°C. The spectrum is shown in Figure 2. The silicon sites are labeled with the conventional Q_n notation. Q_n represents a silicon atom with four potential reactive groups; the n index represents the number of silicon atoms bonded to the first silicon by an oxygen bridging atom. A broad peak was observed, with a maximum at -101 ppm and two shoulders at -94 and -109 ppm, assigned to Q_3 , Q_2 , and Q_4 species, respectively.^{17–19} No peak corresponding to Q_1 was observed. The proportion of Q_n was determined by quantitative analysis based on the peak areas of each species obtained after a deconvolution method. The results show that Q_3 was the major structure, then Q_2 and Q_4 with relative proportions equal to 72, 17, and 11%, respectively. The degree of condensation (D_c) was calculated according to the general following relation:

$$D_c = \frac{Q_1 + 2Q_2 + 3Q_3 + 4Q_4}{4} \times 100$$

A D_c value of 73.5% was found for these conditions. Therefore, we were able to conclude that TEOS was not fully condensed after the protocol in solution followed by thermal treatment at 180°C.

In the following characterization step, sample morphology was assessed by different complementary techniques. Upon visual observation, the film looked transparent and optically uniform. Extraction of the hyperbranched polyester from the hybrid film was attempted using THF. The film did not disintegrate and

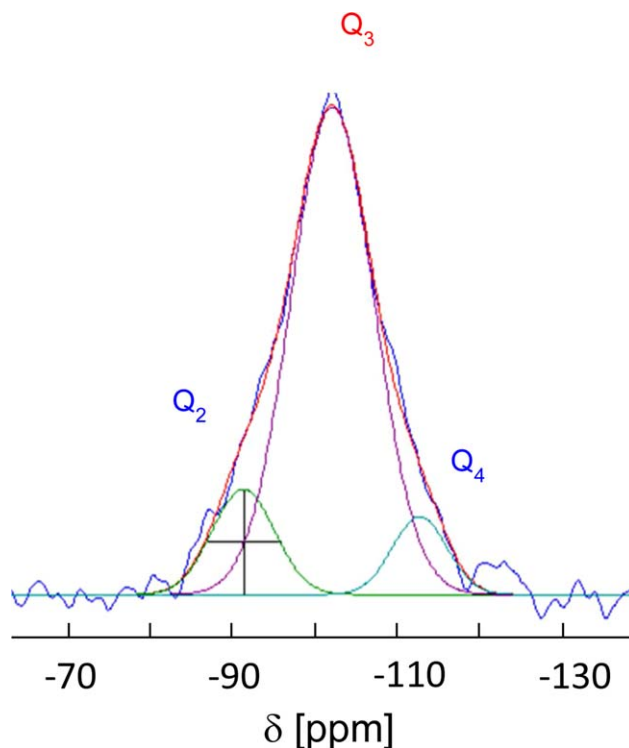


Figure 2. Solid state ²⁹Si NMR of H40-20 hybrid film. [Color figure can be viewed in the online issue, which is available at wileyonlinelibrary.com.]

remained fully cohesive. Only 3 wt % of polymer was extracted. This simple experiment demonstrated that the inorganic phase formed a continuous phase and the polyester was strongly linked to the inorganic component through interfacial interactions because of the difficulty in removing it from the material. The hybrid can be reasonably considered as class II. This structure was confirmed by a calcination test. After degradation of the organic part, the residue obtained was a solid brittle film. This residue was analyzed by TGA and compared to the initial, non calcined H40-20 film. TGA results are depicted in Figure 3. The hybrid material had a maximum degradation temperature at 350°C, corresponding to the degradation of the polyester, and the char content at 700°C was equal to 20 wt %, in perfect agreement with the theoretical value expected from the initial

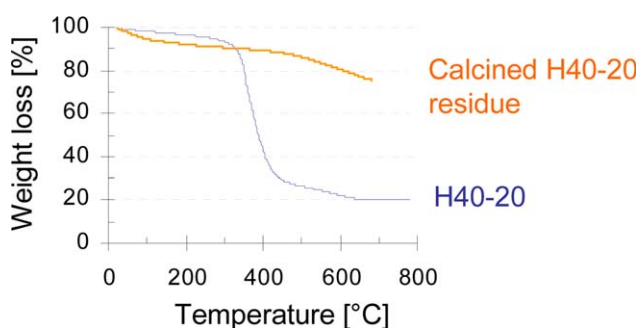


Figure 3. TGA curves for the H40-20 film and calcined film. [Color figure can be viewed in the online issue, which is available at wileyonlinelibrary.com.]

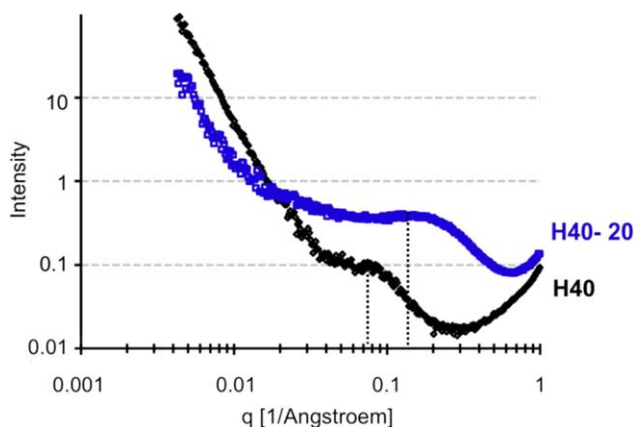


Figure 4. SAXS profiles for the H40 neat hyperbranched polymer and for the H40-20 hybrid material. [Color figure can be viewed in the online issue, which is available at wileyonlinelibrary.com.]

composition. The calcined residue showed no mass loss in the polyester degradation temperature range, confirming full organic phase degradation during thermal treatment at 300°C. The residue obtained was inorganic.

Figure 4 illustrates the SAXS profiles $I(q)$ in a log-log plot, called Porod plot, corresponding to the H40 neat hyperbranched polymer and the H40-20 hybrid material. SAXS has been widely used for the structural characterization of hybrid materials.^{11,25,28} The diffusion profile is decomposed in two classical regimes: a decreasing linear regime at low- q range whose lower and upper limits change with the material composition and an interference peak located at higher- q range. In the wave vector range $0.004 \text{ \AA}^{-1} < q < 0.03 \text{ \AA}^{-1}$, the H40 polymer scattering intensity exhibited power law decay. A correlation peak was observed at 0.07 \AA^{-1} . For spherical-like objects like hyperbranched polymers, the radius of a sphere r is determined as $r = 5.76/q_{\text{max}}$. A correlation distance of $r = 8 \text{ nm}$ was found, corresponding to the size of the HB molecules. The hybrid material SAXS profile showed different characteristic regions. The slope of the linear region in the Porod plot is related to the fractal nature of the inorganic domains; the slope was found equal to -1.5 , indicating the formation of a diffuse interface while a slope in the range from -3 to -4 would have been significant of more dense and smooth particles having a sharp interface. At higher wave vector, a sort of plateau in the scattering profile, was observed for $0.03 \text{ \AA}^{-1} < q < 0.1 \text{ \AA}^{-1}$. Above $q = 0.127 \text{ \AA}^{-1}$, the intensity continued to decrease with q ; the correlation peak observed at $q = 0.127 \text{ \AA}^{-1}$ corresponds to a structural object with a size of $d = 4.5 \text{ nm}$.

TEM images did not reveal any characteristic features; no distinct aggregates or particles could be seen, confirming previous experimental observations. The resulting morphology was very fine, below a few nanometers.

Dynamic mechanical analysis was performed on the neat HB polyester and the corresponding hybrid H40-20. The spectra of these two samples are shown in Figure 5. First, it is worth noting the poor mechanical behavior of the neat hyperbranched polymer: its main α relaxation, corresponding to the glass transition phenomena, was close to room temperature. Simultane-

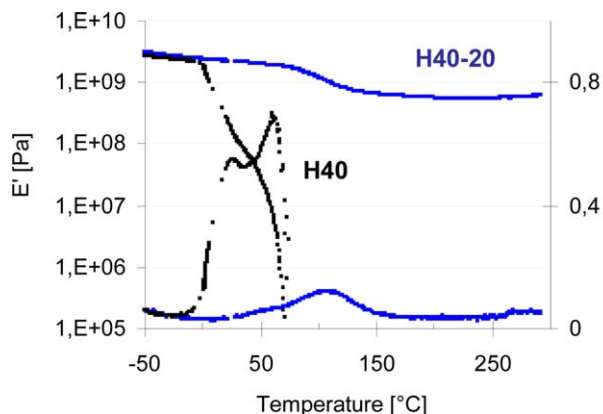


Figure 5. Variation of E' and $\tan \delta$ vs. temperature for the H40 neat hyperbranched polyester and for the H40-20 hybrid material. [Color figure can be viewed in the online issue, which is available at wileyonlinelibrary.com.]

ously, a strong drop in the storage modulus was observed, immediately followed by polymer flow. The thermo-mechanical behavior of the hybrid material was totally different when the silica phase was generated. The α transition shifted to a higher temperature with a maximum at $T_{\alpha} = 110^{\circ}\text{C}$, and its magnitude was strongly decreased. In addition, a significant broadening of the α relaxation peak revealed a wider distribution of relaxation time, corresponding to more or less mobile HB polyester chains. The storage modulus E' showed only a slight decrease in the T_{α} region and a plateau was observed at a high temperature, which means that a crosslinked material was formed. At $T = 200^{\circ}\text{C}$, E' was equal to 620 MPa, which is a remarkably high value. According to this value, which is typical of a glassy material, one can conclude the existence of an inorganic-rich continuous phase. Both, the increase in T_{α} and in modulus resulted from strong interactions created between the organic and inorganic components and the existence of diffuse nanostructures which reduce the motion of polyester chains.^{12,24}

The morphology that developed in the hybrid material synthesized from the H40 hyperbranched polymer and TEOS was different from those reported in the literature in relatively similar systems. In a study published by Zou et al.,¹⁹ hybrids were based on an aliphatic hyperbranched polyester (H20) modified by a coupling agent, GPTMS, in order to obtain a functionalized HB polymer with silane end groups; then, this modified HB polymer was condensed with prehydrolyzed TEOS (using HCl as the catalyst in an ethanol solution).¹⁹ Transparent and hard materials at room temperature were obtained after heating for 24 h at 120°C. The degree of condensation was close to 83% and the gel content was close to 92%. Scanning electron microscopy images showed nanoparticles of colloidal silica 6–9 nm in size. The maximum T_g (DSC) was 72°C.

In contrast to the study by Zou, the TEOS hydrolysis in our protocol was performed in the presence of the hyperbranched polyester. Under the acidic conditions used, hydrolysis of TEOS is very fast and interactions between the $-\text{OH}$ groups of the hyperbranched polyester and silanol groups from the hydrolyzed TEOS are largely promoted. These interactions occur via

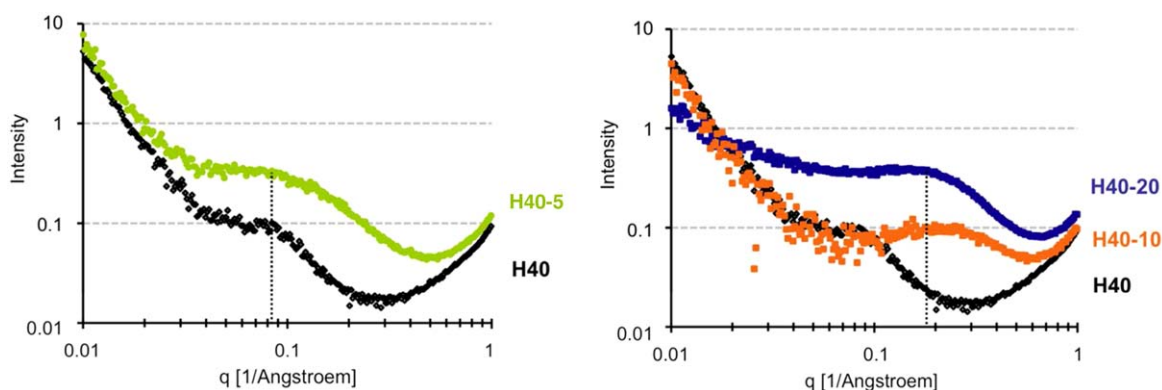


Figure 6. SAXS profiles of the hybrid films containing various amounts of the inorganic phase: 0, 5, 10, and 20 wt %. [Color figure can be viewed in the online issue, which is available at wileyonlinelibrary.com.]

hydrogen bonding between the numerous polyester hydroxyl end groups or via possible hydroxyl group condensation. Following this route, great compatibility between the two phases is achieved and no phase separation with silica particle formation is observed.

Effect of the TEOS Content

The influence of the inorganic content was investigated. O/I hybrid materials containing a theoretical content of 5 and 10 wt % SiO_2 were synthesized and compared to the H40-20 film containing 20 wt % SiO_2 .

^{29}Si solid state NMR recorded on the H40-10 film showed that the Q_3 species was the major ones, while Q_2 and Q_4 were found in smaller amounts. The overall condensation degree, D_c , was 75.5% for this film, with a molar proportion of 21, 52, and 26% for Q_2 , Q_3 , and Q_4 , respectively. The D_c value was in the same range as in the H40-20 film, with less Q_3 species but more Q_2 and Q_4 species. It was not possible to perform such a calculation for the H40-5 hybrid because the signal was too weak.

The hybrid films were homogeneous and optically transparent. After immersion in THF, the H40-10 film remained cohesive while the H40-5 film lost its integrity and was partially dissolved in the solvent. This experiment revealed a clear difference in the morphology of the two hybrid samples. The amount of extracted polyester was 20 and 56 wt % for H40-10 and H40-5, respectively. This decreased with the inorganic phase amount and emphasizes that the interactions between the two phases are more numerous and/or stronger when the silica content is high. A calcination test was also done; after complete polyester degradation, the two films remained cohesive and transparent regardless of the inorganic content. The continuous phase was clearly silica in both cases. It seems *a priori* contradictory to the results obtained in the solubility test for the film containing the lowest content of silica, H40-5. In this particular case, a post-condensation reaction occurred when the sample was submitted to the calcination test at 300°C , while this chemical reaction cannot occur during the solubility test performed at room temperature. At the end of the thermal treatment at 180°C , all the inorganic species are spatially organized around the hyperbranched polyester and are well-dispersed. However, the degree

of condensation was probably not sufficiently high to lead to a dense and continuous inorganic phase as observed in the other hybrid films (H40-20 and H40-10).

The SAXS profiles are shown in Figure 6. The scattering curve shapes of these samples relate to their different morphologies. For the lowest content of inorganic phase, the $I(q)$ curve of the hybrid was very similar to the curve obtained on the H40 hyperbranched polyester; the same correlation peak at $q = 0.07 \text{ \AA}^{-1}$ was observed, but the main difference was a higher signal intensity (0.35 instead of 0.1) due to the presence of the inorganic phase. Therefore, hyperbranched polyester structuration was not modified by the presence of 5 wt % silica. The $I(q)$ curve for the H40-10 hybrid had some similarity with that obtained for the H40 polymer in the low q region, with the same slope and intensity. However, the behavior above $q = 0.1 \text{ \AA}^{-1}$ was more similar to the H40-20 hybrid; the correlation peak was in the same range, but the intensity was lower due to the lower amount of silica.

Again TEM did not allow the observation of any organic and inorganic microphase separation due to the size of the nanostructures and the diffuse nature of the O/I interface.

The influence of the amount of the inorganic phase on the variation of E' and $\tan \delta$ is shown in Figure 7. Very different

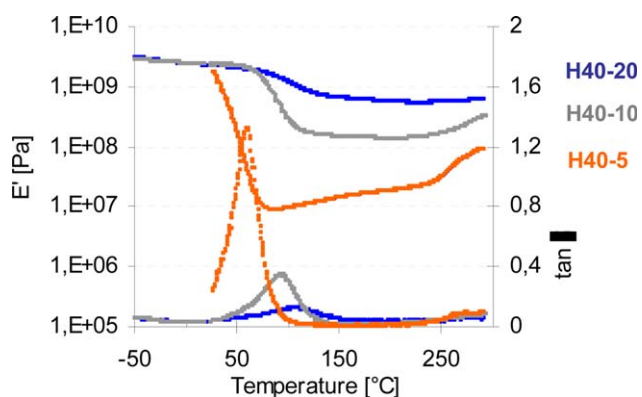


Figure 7. Variation of E' and $\tan \delta$ vs. temperature for the H40-5, H40-10 and H40-20 hybrid materials. [Color figure can be viewed in the online issue, which is available at wileyonlinelibrary.com.]

behaviors were observed. The hybrid containing the lowest inorganic phase content, 5 wt %, behaved like a thermoset material. The glass transition temperature was 60°C, the peak magnitude was high, $\tan \delta_{\max} = 1.3$ and its broadness was weak, i.e., 30°C at mid-height. Therefore, it can be concluded that no strong interactions or confinement effects exist between the two phases because no significant reduction of polyester molecular mobility was observed. The modulus drop was greater than two decades, down to 10 MPa, without polymer flow after T_g compared to the neat polyester. On the contrary, in the rubbery state, a progressive increase in the modulus was noted; it appears that the thermal treatment at 180°C was not long enough to obtain a constant degree of condensation at this temperature. Above 250°C, this increase was even more remarkable; the modulus was equal to 17 MPa at 200°C and 89 MPa at 290°C. This phenomenon is due to post-condensation reactions occurring during the DMA temperature ramp. At the end of the thermal treatment applied for the synthesis of this hybrid material, the continuous phase is the polyester one which is linked by weak interactions to the inorganic phase. Then, upon heating the sample, either in the rheometer or during the calcination test, more post-condensation reactions occur. Therefore, the sample morphology evolves continuously; the inorganic-rich phase becomes more and more dense and connected in order to form a continuous inorganic phase or a cocontinuous phase with the organic-rich phase. The hybrid with a moderate silica content, 10 wt %, showed intermediate DMA behavior compared to the two other samples, containing 5 and 20 wt % silica, regarding both glass transition and modulus changes. Indeed, the glass transition temperature was equal to 90°C, its magnitude was close to 0.3 and its broadness at mid-height was equal to 50°C. The increase in the glass transition temperature, compared to the H40-5 sample, was due to the restriction of polyester macromolecule motion because more and/or stronger interactions between the two phases than those in the 5 wt % hybrid material were created. The decrease in storage modulus was only of one decade and a plateau was clearly observed up to 250°C, a temperature at which a slight modulus increase was noted. The thermal treatment of 4 h at 180°C was enough to reach a stable state of silanol condensation. In agreement with previous solubility and calcination tests, it can be concluded that the morphology of the hybrid material containing 10 wt % silica corresponds to a continuous inorganic phase which is able to develop strong interactions with the polyester hydroxyl terminal groups.

The study of these three different hybrid material compositions showed that different morphologies were developed, depending on the amount of the silica-rich phase generated. In our synthesis conditions, the morphology went from a continuous polyester phase to a continuous silica phase. This phase inversion phenomena was observed for a silica content between 5 and 10 wt %. As a consequence of this morphological modification, both the glass transition temperature and the storage modulus exhibited a considerable increase for the highest inorganic content. In addition, the morphology could be modified by a high temperature post-treatment which allowed post-condensation reactions.

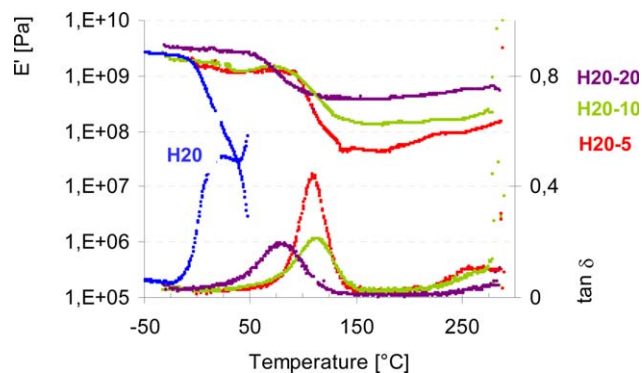


Figure 8. Variation of E' and $\tan \delta$ for the H20-5, H20-10 and H20-20 hybrid materials and the H20-film. [Color figure can be viewed in the online issue, which is available at wileyonlinelibrary.com.]

Effect of Hyperbranched Polyester Molecular Weight

The H20 hyperbranched polyester was used instead of H40 for the synthesis of a new hybrid material series. The H20 molar mass is lower than that of H40, with $M_w = 1700$ and 7300 g mol^{-1} , respectively. Nevertheless, the hydroxyl end group concentration remained in the same range and was theoretically equal to $11.8 \times 10^{-3} \text{ —OH/g}$ and $11.0 \times 10^{-3} \text{ —OH/g}$ for H20 and H40, respectively. Both polymers have a similar glass transition temperature. The synthesis protocol was the same. The amount of TEOS used was calculated in order to obtain 5, 10, and 20 wt % silica in the final hybrid materials (Table I).

The three hybrid materials based on the H20 polyester appeared homogeneous and optically transparent. The solubilization test in THF showed that the three films retained their integrity and remained cohesive which was not the case for the H40-5 hybrid. So, the first influence of the polyester molar mass was noted in the hybrid containing the lowest amount of silica. Indeed, as previously mentioned, the film H40-5 lost its integrity after immersion in THF while that the film H20-5 kept its shape. This observation reveals a difference in film structuration and allows us to suppose that the H20-5 film has a continuous inorganic phase.

TEM images did not reveal any interesting features; no clear organic or inorganic domains could be observed, which confirmed that the resulting morphology was very fine.

Figure 8 shows the temperature dependence of the loss factor and the storage modulus of hybrid materials synthesized from H20 and a different amount of TEOS. The DMA data are tabulated in Table II and compared to the H40 series data. The influence of the silica content in the H20 series was examined first. The storage moduli, above the glass transition region, were clearly increased upon the generation of a higher content of the inorganic phase. At 200°C, there was a difference of one decade between the moduli of the materials synthesized with the lowest and highest amount of silica. The same trend was noted with the hybrids based on H40, although the difference was even higher. The glass transition temperature was the same with the two lowest contents of silica, 5 and 10 wt %, and was equal to 110°C, while a decrease was observed as the amount of silica reached 20 wt %. This last result is the opposite of that

Table II. Dynamic Mechanical Properties of the Different Hybrid Materials

	Boltorn® H20	H20-5	H20-10	H20-20
$E'_{200^{\circ}\text{C}}$ (MPa)	-	57	140	460
T_{α} ($^{\circ}\text{C}$)	23	109	110	69
$L_{1/2}$ (K)	-	30	39	57
	Boltorn® H40	H40-5	H40-10	H40-20
$E'_{200^{\circ}\text{C}}$ (MPa)	-	17	116	620
T_{α} ($^{\circ}\text{C}$)	25	60	90	110
$L_{1/2}$ (K)	-	30	49	95

T_{α} : temperature at the maximum of $\tan \delta$ peak, $L_{1/2}$: width at half-height of the $\tan \delta$ peak.

obtained previously on the H40-20 film, which showed the highest T_{α} of the series. In addition, the $\tan \delta$ relaxation peak broadness, expressed by $L_{1/2}$ (width at half-height of the $\tan \delta$ peak), was smaller in the H20 series as compared to the H40 series.

A molar mass influence could be also seen. For the highest silica content, both H20-20 and H40-20 hybrids showed an inorganic continuous phase according to the high values of the storage modulus at high temperature. However, the glass transition temperature and the broadness of the $\tan \delta$ relaxation peak were significantly decreased for the hybrids based on H20 as compared to hybrids based on H40. This difference could not be explained by the initial values of the polyester glass transition temperature, which were very close. This is indicative of fewer or weaker interactions developed between the H20 polyester and the inorganic component, and of a less heterogeneous distribution of relaxation times of the polymer chains. For the intermediate content of silica, 10 wt %, the modulus drop above the glass transition was quite similar in both hybrids; this drop was moderate, by about one decade. However, the two hybrids had a 20 K difference in glass transition temperatures; the glass transition temperature of the H20-10 hybrid became higher than that of the H40-10 hybrid. This result is surprising and could be attributed to the fact that the material structuration within the H20-10 hybrid led to a very confined organic phase with the creation of strong interfaces between the polyester and the silica-rich phase. For the lowest silica content, 5 wt %, the modulus drop at the glass transition was higher as compared to the two previous cases. However, the value obtained at 200 $^{\circ}\text{C}$ was high for the H20-5 hybrid and may be related to the existence of an inorganic continuous phase, in agreement with the solubility and calcination tests. The H20-5 inorganic continuum was less dense than that obtained for the H20-10 and H20-20 materials. Above 200 $^{\circ}\text{C}$, an increase in the modulus was observed due to some post-condensation reactions, as reported previously. The glass transition temperature was 110 $^{\circ}\text{C}$. The molar mass influence was especially important when the inorganic phase content was low. It is remarkable to obtain a continuous inorganic phase for such a low TEOS content, as this phase promotes the creation of very strong interactions with the polyester and shifts the glass transition temperature to a very high value compared to the neat polyester.

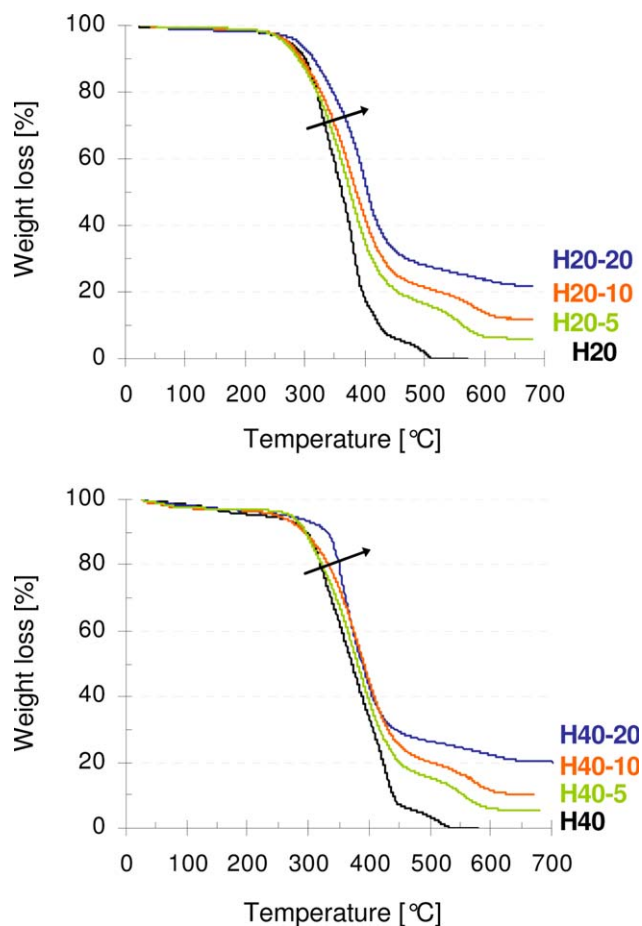


Figure 9. TGA curves of hybrid materials in air (a) H40 based series (b) H20 based series. [Color figure can be viewed in the online issue, which is available at wileyonlinelibrary.com.]

Thermal Stability

Figure 9 displays the TGA thermograms of hybrids with different silica contents, synthesized from either the H40 or H20 polyester. All samples exhibited a one-step decomposition profile in air. The residue at 700 $^{\circ}\text{C}$ was silica since the organic component was likely totally decomposed at this temperature. The values obtained are in agreement with the targeted silica content. The temperature at which 50 wt % of the organic phase was decomposed is reported in Table III. Compared to the neat polymer, H40 or H20, the thermal stability of all hybrid materials was increased. A higher inorganic phase content resulted in greater material thermal stability. In addition, the polyester molar mass also played a more or less pronounced influence, depending on the amount of silica added. The H40 neat polyester was slightly more stable than the H20 neat polyester. Upon addition of the inorganic component, the difference

Table III. Temperature at 50% of Polyester Phase Mass Loss

SiO ₂ wt %	0	5	10	20
$T_{50^{\circ}\text{C}}$ —H40	376	381	388	390
$T_{50^{\circ}\text{C}}$ —H20	359	372	378	394

between the two series was less, and the hybrids behaved very similarly for a silica content of 20 wt %.

CONCLUSIONS

Organic–inorganic hybrid coatings were synthesized based on the sol-gel polymerization of TEOS in the presence of a hyperbranched polyester. Using this very simple process, we obtained a range of homogeneous and transparent O/I materials having a continuous inorganic-rich phase even with a very low initial TEOS content and without the use of any interfacial coupling agent. The development of this morphology was possible thanks to our process in an acidic environment, which favors hydrolysis reactions. As a consequence, strong interactions can be developed at the interface between hydroxyl end groups from the polyester and silanol groups from the hydrolyzed TEOS precursor. No microphase separation occurred even if a nanoscale morphology was generated from a reaction-induced phase separation phenomenon. After thermal treatment at 180°C to perform the condensation reactions, we found that most of the TEOS existed as the Q_3 species. These species underwent post-condensation reactions when the hybrid was heated to a higher temperature. Increasing the TEOS content caused an increase in the glass transition temperature of the organic phase because of the strong interactions created between both phases, which led to a strong reduction in polymer molecular mobility. The storage modulus was increased as well and remained high even at high temperature due to continuous silica-rich phase formation. As a consequence, the thermal stability was also improved. The hyperbranched polyester molar mass showed a strong influence on hybrid morphology and properties. Indeed, using a low polyester molar mass, the highest glass transition temperature, $T_g \sim 110^\circ\text{C}$, was obtained for the two lowest silica contents, 5 and 10 wt %, while using the high polyester molar mass, the highest $T_g \sim 100^\circ\text{C}$ was reached for the highest silica content of 20 wt %.

ACKNOWLEDGMENTS

The authors acknowledge the financial support of FUI (Fonds Uniques Interministeriels) through the DURAMAT project and Dr Libor Matejka from the Institute of Macromolecular Chemistry in Prague (CZ) for his help in the SAXS measurements.

REFERENCES

1. Kickelbick, G. *Hybrid Materials, Synthesis, Characterization, and Applications*; Wiley-VCH: Germany, 2007.
2. Messersmith, P. B.; Giannelis, E. P. *Chem. Mater.* **1994**, *6*, 1719.
3. Barthel, H.; Dreyer, M.; Gottscalk-Gaudig, T.; Litinov, V.; Nikitina, E. *Macromol. Symp.* **2002**, *187*, 573.
4. Jacquolot, E.; Galy, J.; Gérard, J. F.; Roche, A.; Chevet, E.; Fouissac, E.; Verchère, D. *Prog. Org. Coat.* **2002**, *966*, 86.
5. Breuer, O.; Sundararaj, U. *Polym. Compos.* **2004**, *25*, 630.
6. Kuo, S. W.; Chang, F. C. *Prog. Polym. Sci.* **2011**, *36*, 1649.
7. Bizet, S.; Galy, J.; Gérard, J. F. *Macromolecules* **2006**, *39*, 2574.
8. Brinker, C. J.; Scherer, G. W. *Sol-Gel Science. The Physics and Chemistry of Sol-Gel Processing*; Academic Press: San Diego, 1990.
9. Schubert, U.; Hüsing, N.; Lorenz, A. *Chem. Mater.* **1995**, *7*, 2010.
10. Wen, J.; Wilkes, G. L. *Chem. Mater.* **1996**, *8*, 1667.
11. Matejka, L.; Dukh, O.; Meissner, B.; Hlavata, D.; Brus, J.; Strachota, A. *Macromolecules* **2003**, *36*, 7977.
12. Benes, H.; Galy, J.; Gérard, J. F.; Plestil, J.; Valette, L. *J. Sol-Gel Sci. Technol.* **2011**, *59*, 598.
13. Young, S. K.; Gemeinhardt, G. C.; Sherman, J. W.; Storey, R. F.; Mauritz, K. A.; Schiraldi, D. A.; Polyakova, A.; Hiltner, A.; Baer, E. *Polymer* **2002**, *43*, 6101.
14. Sanchez, C.; Ribot, F. N. *J. Chem.* **1994**, *18*, 1007.
15. Frings, S.; Meinema, H. A.; van Nostrum, C. F.; van der Linde, R. *Prog. Org. Coat.* **1998**, *33*, 126.
16. Frings, S.; van Nostrum, C. F.; van der Linde, R. *J. Coat Technol.* **2000**, *72*, 83.
17. Hsu, Y. G.; Chiang, I. L.; Lo, J. F. *J. Appl. Polym. Sci.* **2000**, *78*, 1179.
18. Arkhireeva, A.; Hay, J. N.; Lane, J. M.; Manzano, M.; Masters, H.; Oware, W.; Shaw, S. J. *J. Sol-Gel Sci. Technol.* **2004**, *31*, 31.
19. Zou, J.; Shi, W.; Hong, X. *Compos. A* **2005**, *36*, 631.
20. Zou, J.; Zhao, Y.; Shi, W.; Shen, X.; Nie, K. *Polym. Adv. Technol.* **2005**, *16*, 55.
21. Nebioglu, A.; Teng, G.; Soucek, M. D. *J. Appl. Polym. Sci.* **2005**, *99*, 115.
22. Chen, Y.; Zhou, S.; Chen, G.; Wu, L. *Prog. Org. Coat.* **2005**, *54*, 120.
23. Zhao, Y.; Zou, J.; Shi, W.; Tang, L. *Microporous Mesoporous Mater.* **2006**, *92*, 251.
24. Amerio, E.; Sangermano, M.; Malucelli, G.; Priola, A.; Rizza, C. *Macromol. Mater. Eng.* **2006**, *291*, 1287.
25. Di Gianni, A.; Trabelsi, S.; Rizaz, G.; Sangermano, M.; Althues, H.; Kaskel, S.; Voit, B. *Macromol. Chem. Phys.* **2007**, *208*, 76.
26. Houel, A. Thesis, INSA Lyon, 2011-ISAL-0036.
27. El Kadib, A.; Katir, N.; Bousmina, M.; Majoral, J. P. N. *J. Chem.* **2012**, *36*, 241.
28. Guinier, A.; Fournet, G. *Small Angle Scattering of X-rays*; Wiley: New York, 1955.